JCTC Journal of Chemical Theory and Computation

ARTICLE

pubs.acs.org/JCTC

# Computing Alchemical Free Energy Differences with Hamiltonian Replica Exchange Molecular Dynamics (H-REMD) Simulations

Yilin Meng,[†] Danial Sabri Dashti,[‡] and Adrian E. Roitberg[*,§]

[†]Department of Biochemistry and Molecular Biology, University of Chicago, Chicago, Illinois 60637

[‡]Department of Physics and Quantum Theory Project, University of Florida, Gainesville, Florida 32611-8435

[§]Department of Chemistry and Quantum Theory Project, University of Florida, Gainesville, Florida 32611-8435

**ABSTRACT:** Alchemical free energy calculations play a very important role in the field of molecular modeling. Efforts have been made to improve the accuracy and precision of those calculations. One of the efforts is to employ a Hamiltonian replica exchange molecular dynamics (H-REMD) method to enhance conformational sampling. In this paper, we demonstrated that the H-REMD method not only improves convergence in alchemical free energy calculations but also can be used to compute free energy differences directly via the Free Energy Perturbation (FEP) algorithm. We show a direct mapping between the H-REMD and the usual FEP equations, which are then used directly to compute free energies. The H-REMD alchemical free energy calculation (replica exchange free energy perturbation, REFEP) was tested on predicting the p$K_a$ value of the buried Asp26 in thioredoxin. We compare the results of REFEP with TI and regular FEP simulations. REFEP calculations converged faster than those from TI and regular FEP simulations. The final predicted p$K_a$ value from the H-REMD simulation was also very accurate, only 0.4 p$K_a$ units above the experimental value. Utilizing the REFEP algorithm significantly improves conformational sampling, and this in turn improves the convergence of alchemical free energy simulations.

## INTRODUCTION

Free energy, especially the free energy difference between two states, is a crucial quantity in the study of chemical and biological systems.[1] Knowledge of the free energy differences can help us understand the behaviors of such systems. For example, the free energy of binding is one of the criteria used to evaluate the performance of drugs.[2] Therefore, one important aspect of molecular modeling is to yield accurate free energy differences efficiently. Many free energy calculation methodologies (such as free energy perturbation,[3] thermodynamic integration,[4] umbrella sampling,[5−7] and Jarzynski's equality[8]) as well as analysis techniques (such as the weighted histogram analysis method[9] and Bennett acceptance ratio method[10,11]) have been developed to achieve this goal. In general, free energy calculations could be divided into alchemical free energy and conformational free energy calculations. The alchemical free energy calculations are often employed when studying the free energy differences of processes that involve changes in noncovalent interactions. In an alchemical free energy simulation, a nonphysical reaction coordinate $\lambda$ is generally adopted in order to connect the initial and final states. This reaction coordinate is usually expressed as an interpolation of the initial and final states. Thus, an alchemical process is achieved through a series of intermediate states having no direct physical meaning. Since the free energy difference between two states is a state function, the actual choice of coordinate cannot, in the limit of infinite sampling, affect qthe results. Free energy perturbation (FEP) and thermodynamic integration (TI) are two common methodologies that are utilized in alchemical free energy computations.

One important issue in alchemical free energy calculations is the convergence of the free energy difference versus computational cost. The convergence is particularly difficult in systems involving slow structural transition or large environmental reorganization as $\lambda$ changes.[12−14] Therefore, conformational sampling is crucial in alchemical free energy calculations. Enhanced sampling methods, such as replica exchange molecular dynamics (REMD),[15] orthogonal space random walk (OSRW),[14] and accelerated molecular dynamics (AMD)[16] have been applied to free energy simulations in order to accelerate conformational sampling and, in turn, to yield accurate and converged free energy differences. Among the enhanced sampling methodologies, the REMD method is of particular interest because the weight of each state is a priori known (Boltzmann factor). The REMD algorithm was initially introduced by Sugita and Okamoto in 1999. In their REMD algorithm, $N$ noninteracting copies (replicas) of a system are simulated at $N$ different temperatures (one each). Regular MD is performed, and periodically an exchange of configurations between two (usually adjacent) temperatures is attempted. Many variants of the original REMD method have been developed. One of them is the so-called "Hamiltonian REMD (H-REMD)".[17−20] In the H-REMD algorithms, replicas differ in their potential energies but (usually) have the same temperature. In practice, different ways of assigning the potential energy function to replicas have been developed. For example, Fukunishi et al.[17] scaled hydrophobic interactions and van der Waals interactions. Protein−water as well as water−water interactions are scaled in the replica exchange with solute tempering (REST) algorithm.[18] Coarse-grained potential energy functions (low resolution) are combined with

**Received:** March 3, 2011
**Published:** July 28, 2011

all-atom force fields (high resolution) in the resolution REMD algorithm.[19−21]

Both temperature-based and Hamiltonian-based REMD have been applied to alchemical free energy calculations. Woods et al.[13,22] and Rick[23] have combined the temperature-based REMD with TI calculation. A temperature-based REMD simulation is conducted at each state along the reaction coordinate. Woods et al.[13,22] have also applied the H-REMD methodology to FEP and TI calculations. Each replica in the H-REMD simulation represents a state along the reaction coordinate $\lambda$, and a periodic swap in $\lambda$ is attempted. Relative solvation free energy of water and methane as well as the relative binding free energies of halides to calis[4]pyrrole have been calculated in this way.[22] The Yang group has developed a dual-topology alchemical H-REMD (DTA-HREM) method.[24] Their method was tested on the free energy of mutating an asparagine amino acid (with two ends blocked) to leucine. More recently, the Roux group coupled the FEP methodology with the distributed replica technique (REPDSTR).[25,26] An additional acceleration in the sampling of the side-chain dihedral angle was also incorporated when Jiang and Roux utilized the FEP/H-REMD method to study the absolute binding free energy of *p*-xylene to the T4 lysozyme L99A mutant.[26] In all of those studies, the conformational sampling and convergence of free energy computations showed significant improvement when the REMD method was applied. The protocol presented here accelerates convergence but, of course, does not solve know problems in the field related to enhanced sampling of coordinates orthogonal to $\lambda$ space, which would hamper many of the current methods.

In this paper, we will demonstrate that FEP is actually already incorporated in the H-REMD method in an elegant and formal way. The REFEP method is shown to be not only an enhanced sampling method but also a free energy calculation algorithm. We will apply the REFEP method to the p$K_a$ prediction of thioredoxin Asp26. The experimental p$K_a$ value of 7.5 has been shown to be one of the largest shifted from the intrinsic p$K_a$ value[27,28] and, hence, makes it an interesting case to be studied theoretically. TI and FEP (regular molecular dynamics for conformational sampling) alchemical free energy simulations have been conducted in order to compare with REFEP simulations. A very accurate theoretical p$K_a$ value is obtained from REFEP simulations. The convergence of the free energy difference and p$K_a$ value is achieved in REFEP simulations much faster than that in the FEP and TI simulations. The advantage and simplicity of using the H-REMD simulation to compute the alchemical free energy difference is clearly shown.

## THEORY AND METHOD

**Free Energy Perturbation (FEP).** The FEP method, which was initially introduced by Zwanzig in 1954,[3] is a well established method and is considered the most frequently employed methodology in alchemical free energy calculations.[12] The details of the FEP, as well as the TI, methodology and its applications have been extensively reviewed.[12,29−32] Therefore, only a very brief description of the FEP and TI methods will be given here. Consider two states (1 and 2) of a system in the canonical (NVT) ensemble, and their corresponding Helmholtz free energies $A_1$ and $A_2$. The Helmholtz free energy difference between two states can be expressed as

$$\Delta A_{1\rightarrow 2} = -k_B T \ln\langle e^{-[U_2(q) - U_1(q)]/k_B T}\rangle_1 \quad (1)$$

Here, $k_B$ is the Boltzmann constant, $T$ is the temperature, and $q$ is the molecular structure. $U_1$ and $U_2$ are the potential energies of states 1 and 2, respectively. The bracket with subscript 1 stands for the average calculated over the structural ensemble generated by state 1. In order to compute $\Delta A_{1\rightarrow 2}$, one simulation of state 1 is performed. Once a configuration $q$ is taken, the potential energy difference at configuration $q$ is computed. The ensemble average, which is $\langle e^{-[U_2(q)-U_1(q)]/k_B T}\rangle_1$, can be calculated easily, and hence, $\Delta A_{1\rightarrow 2}$ is obtained. Although the Helmholtz free energies are utilized here, eq 1 can be extended to an isothermal−isobaric (NPT) ensemble and to the Gibbs free energy in the same manner.

When the fluctuations in $\Delta U$ in eq 1 are too large, FEP calculations are notoriously hard to converge. The convergence of the FEP calculation will be poor if the overlap in phase space between the two states is small. In order to compute the free energy difference between two states that are very different, intermediate states mixing the two end points are adopted in such a way that the differences between neighbors can be treated as perturbations. A frequently employed method to generate intermediate states is to interpolate potential energy functions linearly, as shown in eq 2. In eq 2, $U_1$ and $U_2$ are the potential energy functions of states 1 and 2, respectively. Free energy differences between neighboring states are then computed. The sum of individual free energy differences will be the targeted free energy difference between states 1 and 2 (eq 3). There are many ways of executing FEP calculations involving intermediate states. The double-ended, double-wide,[30,33] and overlap sampling algorithms[34] are among the most popular ones. A thorough description of different algorithms and their performance can be found in a recent review by Jorgensen and Thomas.[30]

$$U(\lambda) = (1-\lambda)U_1 + \lambda U_2 \quad (2)$$

$$\Delta A_{1\rightarrow 2} = -k_B T \sum_i \ln\langle e^{-(U(\lambda_{i+1}) - U(\lambda_i))/k_B T}\rangle_i \quad (3)$$

In practice, computing $\Delta A_{1\rightarrow 2}$ (forward free energy difference) is equally easy (or hard) as computing $\Delta A_{2\rightarrow 1}$ (backward free energy difference), and one is exactly the opposite of the other in principle. Evaluation of forward and backward free energy differences provides an indication of convergence. Furthermore, the potential energy differences generated from both directions can be utilized to reduce statistical error. The Bennett acceptance ratio (BAR) method is a frequently employed scheme to improve the precision of a free energy estimator.[10−12]

**Thermodynamic Integration (TI).** Another way of writing the free energy difference between two states 1 and 2 is

$$\Delta A_{1\rightarrow 2} = \int_0^1 \left(\frac{\partial A}{\partial \lambda}\right) d\lambda = \int_0^1 \left\langle \frac{\partial U}{\partial \lambda}\right\rangle_\lambda d\lambda \quad (4)$$

Here, $\lambda$ is a reaction coordinate connecting states 1 and 2, and $U$ is the potential energy of a state along the reaction coordinate. The bracket represents an ensemble average generated at a value of $\lambda$. The integration is often evaluated numerically via trapezoidal rule or Gaussian quadrature. If $U(\lambda)$ is constructed as in eq 2, the derivative of $U(\lambda)$ with respect to $\lambda$ is

$$\frac{\partial U(\lambda)}{\partial \lambda} = U_2 - U_1 \quad (5)$$

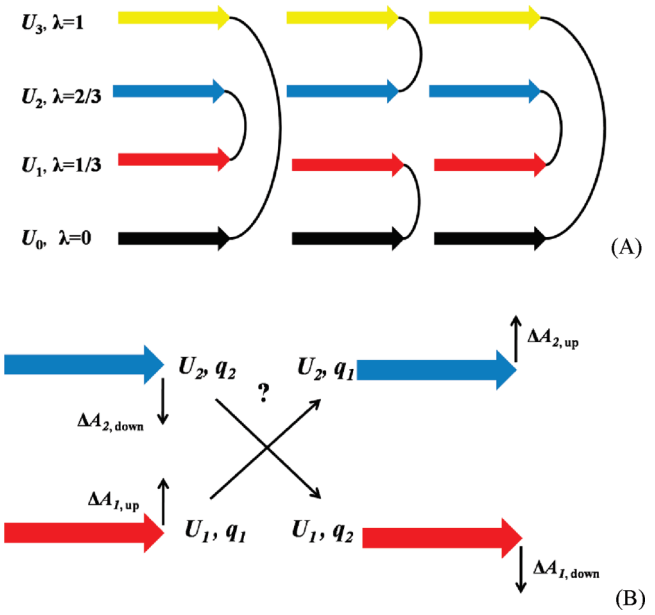


**Figure 1.** Diagrams displaying the H-REMD exchange algorithm and free energy calculation. (A) Exchange attempt orders. Replicas connected by a curve are neighbors, and attempts are made to exchange molecular configurations ($q$). (B) Free energy calculations in the H-REMD method. Each replica has two free energy differences: $\Delta A_{up}$ and $\Delta A_{down}$ from its attempting neighbor form a pair and are computed simultaneously, while $\Delta A_{down}$ and $\Delta A_{up}$ from its attempting neighbor form the other pair. In exchange attempts (regardless if the attempts are accepted or rejected), two pairs of free energy differences are computed in an alternating fashion utilizing eq 1.

And the free energy difference between states 1 and 2 can be expressed as

$$\Delta A_{1\rightarrow 2} = \int_0^1 \langle U_2 - U_1 \rangle_\lambda \, d\lambda \tag{6}$$

Hence, the ensemble average of potential energy gap between states 1 and 2 at each $\lambda$ value is needed in a TI calculation. In this manuscript, we use the term TI to refer to constrained TI, in which the value of $\lambda$ is not allowed to change at each window.

**Hamiltonian Replica Exchange Molecular Dynamics (H-REMD).** The original REMD method utilizes replicas having different temperatures (T-REMD). Replicas at high temperatures overcome potential energy barriers more easily than those at low temperatures. Another way to overcome potential energy barriers is simply to change the potential energy surface to reduce potential energy barriers. In the H-REMD algorithm, replicas differ in their Hamiltonians but have the same temperature. Regular MD is performed, and an exchange of configurations between two neighboring replicas is attempted periodically.

Figure 1 demonstrates the H-REMD algorithm and the free energy computation in an H-REMD simulation. Let us consider two replicas 1 and 2 with corresponding potential energies $U_1$ and $U_2$. By employing the detailed balance condition and Boltzmann weight of each molecular structure, the transition probability can be written as

$$w(q_1 \rightarrow q_2) = \min\{1, e^{-[(U_1(q_2) + U_2(q_1) - U_1(q_1) - U_2(q_2))/k_B T]}\} \tag{7}$$

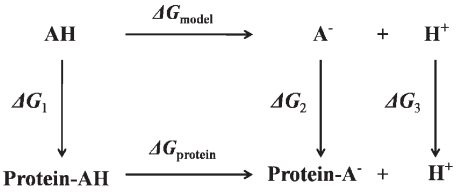


**Figure 2.** Thermodynamic cycle used to compute the p$K_a$ shift. Both acid dissociation reactions occur in aqueous solution. The "protein-AH" represents the ionizable residue in a protein environment. The "AH" represents the model compound which is usually the same ionizable residue with capped terminii. In practice, a proton does not disappear but instead becomes a dummy atom. The proton still has its position and velocity. The bonded interactions involving the proton are still effective. However, there are no nonbonded interactions for that proton. The change in the ionization state is reflected by changes of partial charges in the ionizable residue.

where $q_1$ and $q_2$ are the molecular structures of replicas 1 and 2 before an exchange attempt, respectively. A Monte Carlo–Metropolis criterion[35] is used to evaluate whether the attempted swap of structures between two replicas should be accepted or not.

Equation 7 can be regrouped as

$$w(q_1 \rightarrow q_2) = \min\{1, e^{-[(U_2(q_1) - U_1(q_1) + U_1(q_2) - U_2(q_2))/k_B T]}\} \tag{8}$$

When comparing the exponential terms in eqs 1 and 8, it is clear that eq 8 incorporates all information necessary for a FEP calculation. $U_2(q_1) - U_1(q_1)$ is the potential energy difference computed on the basis of the structural ensemble generated by $U_1$, while $U_1(q_2) - U_2(q_2)$ is the potential energy difference computed on the basis of the structural ensembles generated by $U_2$. Every time the transition probability is computed, those potential energy differences can be utilized to compute the ensemble average shown in eq 1. Therefore, $\Delta A_{1\rightarrow 2}$ and $\Delta A_{2\rightarrow 1}$ can be computed on-the-fly utilizing the double-ended scheme. The ensemble average in eq 1 is computed regardless of whether an exchange attempt is accepted or rejected. When employing the H-REMD method to improve conformational sampling in the study of alchemical changes, H-REMD simulations are able to not only enhance conformational sampling but also yield the free energy difference directly. In fact, a regular FEP calculation can be thought of as an H-REMD calculation where no exchanges are allowed between replicas.

In practice, as shown in Figure 1, there are two free energy difference calculations ($\Delta A_{up}$ and $\Delta A_{down}$) continuosly associated with each replica. Take replica 1 as an example: $\Delta A_{up} = \Delta A_{1\rightarrow 2}$ while $\Delta A_{down} = \Delta A_{1\rightarrow 0}$. In principle, when converged, $\Delta A_{1,up}$ should be equal to the negative of $\Delta A_{2,down}$:

$$\Delta A_{1,up} = -k_B T \ln\langle e^{-(U_2 - U_1)/k_B T}\rangle_1 = -\Delta A_{2,down} = k_B T \ln\langle e^{-(U_1 - U_2)/k_B T}\rangle_2 \tag{9}$$

Any difference (except for the sign) between the two is an indication of error or lack of convergence.

Convergence was gauged also by the time dependence of the predicted free energy differences, computing $\Delta G$ versus simulation length. This provides an asymptotically unbiased estimator for $\Delta G$, and all methods presented here must eventually reach

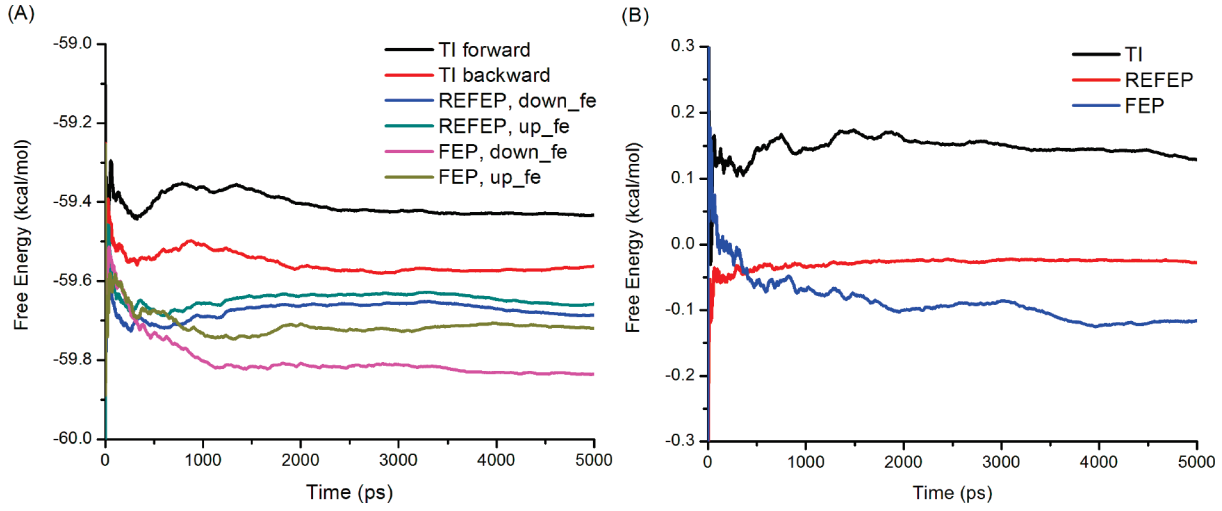


**Figure 3.** (A) Cumulative average free energy differences between protonated and deprotonated aspartic acid in the model compound ($\Delta G$(AH→A$^-$)). (B) The differences between forward and backward $\Delta G$(AH→A$^-$). (C) Cumulative average free energy differences between protonated and deprotonated Asp26 in thioredoxin ($\Delta G$(proteinAH → proteinA$^-$)). (D) The differences between forward and backward(G-(proteinAH → proteinA$^-$).

**Table 1. Free Energy Difference between Protonated and Deprotonated Aspartic Acids Obtained from TI, REFEP, and FEP Alchemical Free Energy Simulations**[a]

| | | TI | REFEP | FEP |
|---|---|---|---|---|
| ASP model | forward | −59.43 (0.06) | −59.69 (0.05) | −59.84 (0.06) |
| compound | backward | −59.56 (0.06) | −59.66 (0.05) | −59.72 (0.06) |
| | average | −59.50 (0.08) | −59.68 (0.08) | −59.78 (0.08) |
| Asp26 in | forward | −54.35 (0.61) | −54.29 (0.17) | −54.23 (0.56) |
| thioredoxin | backward | - 55.82 (0.39) | −54.24 (0.14) | −53.84 (0.56) |
| | average | −55.09 (0.72) | −54.27 (0.22) | −54.04 (0.79) |
| | forward | 5.08 (0.61) | 5.40 (0.18) | 5.61 (0.56) |
| $\Delta G$ difference | backward | 3.74 (0.39) | 5.42 (0.15) | 5.88 (0.56) |
| | average | 4.41 (0.72) | 5.41 (0.23) | 5.74 (0.79) |
| predicted | forward | 7.7 (0.4) | 7.9 (0.1) | 8.1 (0.4) |
| $pK_{a,protein}$ | backward | 6.7 (0.3) | 7.9 (0.1) | 8.3 (0.4) |
| | average | 7.2 (0.5) | 7.9 (0.2) | 8.2 (0.6) |

[a] Free energy differences were calculated by utilizing all data points from a simulation (5 ns for the model compound and 4 ns for Asp26). The $\Delta G$ difference is given by $\Delta G$(proteinAH → proteinA$^-$) − $\Delta G$(AH → A$^-$). All backward free energy differences have positive signs and hence are multiplied by −1. Then, the average values of forward and backward free energy differences were computed and reported here. All free energies have units of kcal/mol. The numbers in parentheses are error bars. The error bars for forward and backward free energy differences of "model compound" and "Asp26 in thioredoxin" were calculated via block averages (a simulation was truncated into five blocks). The rest were obtained by error propagations.

the same final value (within error bars). REFEP is presented in this article as showing faster convergence toward the final value.

**Simulation Details.** Accurately determining the p$K_a$ values of ionizable residues, especially those with large shifts from intrinsic p$K_a$ values, is of great interest both experimentally and computationally.[27,28,36] In this paper, the p$K_a$ calculation of Asp26 in thioredoxin has been selected as a test case in order to compare the performance of alchemical free energy simulations. Asp26 has been found deeply buried in thioredoxin and possesses one of the largest p$K_a$ shifts among protein carboxylic groups.[27,28] Following the protocol employed in the paper of Simonson et al.,[36] the thermodynamic cycle utilized to compute the p$K_a$ value of an ionizable residue is given in Figure 2. As can be seen in Figure 2, the use of a model compound as an auxiliary leg in the thermodynamic cycle makes $\Delta G_3$ (proton to proton) equal to zero. Essentially, the p$K_a$ shift relative to the intrinsic value (p$K_{a,model}$) is computed as

$$pK_a(\text{protein}) = pK_a(model) + \frac{1}{2.303k_BT}[\Delta G(\text{proteinAH} \rightarrow \text{proteinA}^-) - \Delta G(\text{AH} \rightarrow \text{A}^-)] \quad (10)$$

where $\Delta G$(proteinAH → proteinA$^-$) and $\Delta G$(AH → A$^-$) are the free energy differences between protonated and deprotonated aspartic acid in the protein environment and in aqueous solution, respectively. Alchemical free energy simulations were performed in order to yield those two terms. In eq 10, the Gibbs free energy differences are used because experiments determining p$K_a$ values are generally conducted under an isobaric−isothermal condition.

Aspartic acid dipeptide in implicit water solvent was taken as the model compound with a p$K_a$ value taken as 4.0.[37] The oxidized form of thioredoxin (PDB code 2TRX)[38] in implicit water was used in our simulation. Changes in ionization were represented by changes in the partial charges of the aspartic acid side chain (ASH→ASP in the AMBER terminology). Since the van der Waals radius of the proton in aspartic acid is zero for both protonated and deprotonated species, the free energy difference only contains the electrostatic interactions.

Three types of free energy simulations have been performed for both the model compound and the protein: TI (forward and backward), H-REMD-FEP (REFEP), and regular FEP simulations. Our regular FEP simulations were carried out via H-REMD simulations but with all exchange attempts rejected. Comparing the p$K_a$ prediction and free energy convergence from FEP and REFEP simulations will directly indicate the effect of the

enhanced conformational sampling due to the exchanges. Linear interpolation of point charges was carried out in order to assign side chain charges for intermediate states. A seven-point Gaussian quadrature has been selected to compute total free energy difference for TI calculations. Therefore, eight $\lambda$ values (one end point is needed in either direction) were utilized in the TI simulation. Due to the implementation of the TI algorithm in AMBER, 16 replicas were utilized to ensure the same amount of simulation time for all free energy simulations. A simulation time of 5 ns was used for each $\lambda$ value and for each replica in the study of the model compound, while for thioredoxin, we used 4 ns runs. Structural swaps between neighboring replicas were attempted every 2 ps (1000 MD steps). No particular attempt was made in this work to optimize the number or location of the replicas, nor the exchange attempt frequency. Work in this area is in progress.

All simulations were done using the AMBER 10 molecular simulation suite,[39] locally modified to add H-REMD/REFEP capabilities. The AMBER ff99SB force field[40] was utilized in all of the simulations. The SHAKE algorithm[41] was used to constrain the bonds connecting hydrogen atoms with heavy atoms in all of the simulations, which allowed the use of a 2 fs time step. The OBC (Onufriev, Bashford, and Case) generalized Born implicit solvent model (*igb* = 5 in the AMBER terminology)[42] was used to model the water environment in all of our calculations. The cutoff for nonbonded interaction and the Born radii was set to 99 Å. This value is larger than the dimension of both systems. Langevin dynamics was employed in order to maintain the temperature at 300 K, using a friction coefficient of 3.0 $ps^{-1}$.

## RESULTS AND DISCUSSIONS

**Acceptance Ratio of H-REMD Simulations.** The accuracy of FEP depends on the overlaps between phase spaces, which can be measured as overlaps between potential energy difference distributions.[12] The acceptance ratio in an H-REMD simulation is an indication of the overlap between two potential energy difference distributions.[24] Therefore, it could be utilized to monitor the convergence of free energy calculation qualitatively. In our study, large acceptance ratios were observed in both the model compound and protein H-REMD simulation. The acceptance ratio between two neighbors ranged from 0.7 to 0.9 in all H-REMD simulations. Those large acceptance ratios indicate that the overlap in phase space is large.

**Aspartic Acid Model Compound Study.** The free energy differences on the right-hand side of eq 10 were calculated as described in the Theory and Method section. The cumulative average free energy difference as a function of time is reported here. Figure 3A shows the $\Delta G(AH \rightarrow A^-)$ from TI, H-REMD, and FEP simulations (as mentioned before, a FEP simulation has been performed by rejecting all exchange attempts in an H-REMD simulation). The differences between forward and backward $\Delta G(AH \rightarrow A^-)$ are shown in Figure 3B. A converged alchemical free energy simulation should generate the same forward and backward free energy numerically (except for an opposite sign). Any nonzero value is an indication of free energy not converged.

For a simple system such as aspartic acid in implicit water, 5 ns of simulation time was long enough for $\Delta G(AH \rightarrow A^-)$ to stabilize in all three alchemical free energy simulations, as shown in Figure 3A. The forward and backward $\Delta G(AH \rightarrow A^-)$ at the end of each free energy calculation and the corresponding error bars are listed in Table 1. The forward and backward free energy differences are the same (within error bars) for both REFEP and FEP simulations. However, the TI simulations failed to do that, although the difference was very small (the difference between forward and backward $\Delta G(AH \rightarrow A^-)$ was only 0.13 kcal/mol). The average of forward and backward $\Delta G(AH \rightarrow A^-)$ was taken as the final value of $\Delta G(AH \rightarrow A^-)$ for the model compound and is also reported in Table 1. Clearly, as shown in Figure 3B, the REFEP simulations have converged much faster than the FEP calculations did.

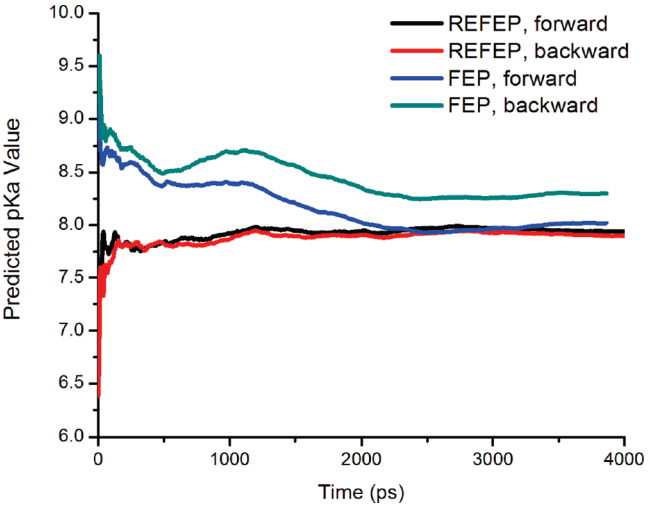


**Figure 4.** Predicted $pK_a$ value of Asp26 in thioredoxin as a function of time. The ($\Delta G(AH \rightarrow A^-)$ values utilized in eq 10 were −59.68 and −59.78 kcal/mol for REFEP and FEP, respectively. The experimental value is 7.5.

**Study on Asp26 in Thioredoxin.** The free energy difference between protonated and deprotonated Asp26 is shown in Figure 3C and D. By analogy with the model compound plots, the cumulative average as a function of time is reported. The cumulative average was clearly not converged during the TI simulation, and neither was the difference between forward and backward $\Delta G(\text{proteinAH} \rightarrow \text{proteinA}^-)$. According to Table 1, after 4 ns of TI simulation, the difference between forward and backward free energy was 1.4 kcal/mol, while the uncertainty of the forward and backward free energy differences was 0.61 and 0.39 kcal/mol, respectively. Data not presented here show that TI requires roughly 40 ns of dynamics before converging to results comparable with FEP/REFP. It is worth noting that this comparison is slightly unfair to TI and deserves further explanation. First, we used eight intermediate states for TI versus 16 for FEP/REFEP. This setup, when executed within Amber, uses the same CPU time since the TI implementation is done with dual-topology methods. In fact, reusing the ensemble generated with the FEP Hamiltonians and computing TI values on that ensemble produces very fast-converging results.

For regular FEP free energy calculations, the cumulative averages stabilized after roughly 2.2 ns of simulation, while the cumulative averages for the REFEP simulation stabilized much faster (shown in Figure 3C). Furthermore, Figure 3D illustrates that the difference between forward and backward $\Delta G(\text{proteinAH} \rightarrow \text{proteinA}^-)$ in the REFEP reached a value very close to zero (~0.05 kcal/mol) very quickly. As described previously, the final value of $\Delta G(\text{proteinAH} \rightarrow \text{proteinA}^-)$ was calculated as the average of forward and backward free energy differences. Although the final free energy differences

computed from 4 ns of simulation were the same for REFEP and regular FEP, the calculations converged much faster in REFEP than in FEP simulation. Since the H-REMD and FEP calculations only differed in whether structures were allowed to be exchanged or not, the improvement in alchemical free energy convergence resulted from employing enhanced conformational sampling technique is significant. Data not presented here show that the histograms of $P_1(\Delta U)\exp(-\beta(\Delta U))$ for the calculation of the free energy difference between replicas 1 and 2 for different sampling times are slightly different for FEP and REFEP. The REFEP distributions converge faster with time and sample the left side of the distribution better. This helps rationalize the faster convergence of our technique.

**p$K_a$ Prediction for Asp26 in Thioredoxin.** The p$K_a$ value of Asp26 in thioredoxin can be computed by eq 10. The final value of $\Delta G(\text{proteinAH} \rightarrow \text{proteinA}^-)$ from the REFEP simulation was −54.3 kcal/mol, with a predicted p$K_a$ value of 7.9, which is only 0.4 p$K_a$ units above the experimental value. The predicted p$K_a$ value with respect to time from REFEP simulations was plotted in Figure 4 in order to demonstrate the convergence of the p$K_a$ prediction. Figure 4 shows that REFEP simulations not only yielded an accurate predicted p$K_a$ value but also achieved convergence very fast. The regular FEP simulation predicted a p$K_a$ value of 8.2, which is 0.7 p$K_a$ units above the experimental value. The convergence in the regular FEP simulation was also worse than that in the REFEP simulation.

## CONCLUSIONS

Conformational sampling is crucial in free energy calculations. In the case of alchemical free energy calculations, H-REMD is a useful and popular method to enhance the accuracy and convergence of free energy simulations. In this paper, we have demonstrated that REFEP not only improves conformational sampling in free energy calculations but also yields a free energy difference directly via the FEP algorithm. The implementation of REFEP is trival, once a H-REMD code is in place. The REFEP alchemical free energy calculation was tested on predicting the p$K_a$ value of Asp26 in thioredoxin and compared with TI and regular FEP simulations. Free energy differences from the REFEP simulation converged faster than those from TI and regular FEP simulations. The final predicted p$K_a$ value from the REFEP simulation was very accurate, only 0.4 p$K_a$ unit above the experimental value. Utilizing the REFEP algorithm significantly improves conformational sampling, and this in turn improves the convergence of alchemical free energy simulations.

## AUTHOR INFORMATION

### Corresponding Author

*E-mail: roitberg@ufl.edu.

## ACKNOWLEDGMENT

This work is supported from National Institute of Health under contract 1R01AI073674. Partial funding was provided by NSF award 1047919 to A.E.R. Computer resources and support were provided by the Large Allocations Resource Committee through grant TG-MCA05S010 and the University of Florida High-Performance Computing Center. We thank the reviewers for extremely useful comments that have made this manuscript better.

## REFERENCES

(1) *Free energy calculations. Theory and applications in chemistry and biology*; Chipot, C., Pohorille, A., Eds.; Springer Verlag: Berlin, 2007.
(2) Bash, P. A.; Singh, U. C.; Brown, F. K.; Langridge, R.; Kollman, P. A. *Science* **1987**, *235*, 574–576.
(3) Zwanzig, R. W. *J. Chem. Phys.* **1954**, *22*, 1420–1426.
(4) Kirkwood, J. G. *J. Chem. Phys.* **1935**, *3*, 300–313.
(5) Mezei, M. *J. Comput. Phys.* **1987**, *68*, 237–248.
(6) Roux, B. *Comput. Phys. Commun.* **1995**, *91*, 275–282.
(7) Torrie, G. M.; Valleau, J. P. *J. Comput. Phys.* **1977**, *23*, 187–199.
(8) Jarzynski, C. *Phys. Rev. Lett.* **1997**, *78*, 2690–2693.
(9) Kumar, S.; Bouzida, D.; Swendsen, R. H.; Kollman, P. A.; Rosenberg, J. M. *J. Comput. Chem.* **1992**, *13*, 1011–1021.
(10) Bennett, C. H. *J. Comput. Phys.* **1976**, *22*, 245–268.
(11) Shirts, M. R.; Chodera, J. D. *J. Chem. Phys.* **2008**, *129*, 124105.
(12) Pohorille, A.; Jarzynski, C.; Chipot, C. *J. Phys. Chem. B* **2010**, *114*, 10235–10253.
(13) Woods, C. J.; Essex, J. W.; King, M. A. *J. Phys. Chem. B* **2003**, *107*, 13703–13710.
(14) Zheng, L. Q.; Chen, M. G.; Yang, W. *Proc. Natl. Acad. Sci. U. S. A.* **2008**, *105*, 20227–20232.
(15) Sugita, Y.; Okamoto, Y. *Chem. Phys. Lett.* **1999**, *314*, 141–151.
(16) Hamelberg, D.; Mongan, J.; McCammon, J. A. *J. Chem. Phys.* **2004**, *120*, 11919–11929.
(17) Fukunishi, H.; Watanabe, O.; Takada, S. *J. Chem. Phys.* **2002**, *116*, 9058–9067.
(18) Liu, P.; Kim, B.; Friesner, R. A.; Berne, B. J. *Proc. Natl. Acad. Sci. U. S. A.* **2005**, *102*, 13749–13754.
(19) Liu, P.; Voth, G. A. *J. Chem. Phys.* **2007**, *126*, 045106.
(20) Lyman, E.; Ytreberg, F. M.; Zuckerman, D. M. *Phys. Rev. Lett.* **2006**, *96*, 028105.
(21) Lwin, T. Z.; Luo, R. *J. Chem. Phys.* **2005**, *123*, 194904.
(22) Woods, C. J.; Essex, J. W.; King, M. A. *J. Phys. Chem. B* **2003**, *107*, 13711–13718.
(23) Rick, S. W. *J. Chem. Theory Comput.* **2006**, *2*, 939–946.
(24) Min, D. H.; Li, H. Z.; Li, G. H.; Bitetti-Putzer, R.; Yang, W. *J. Chem. Phys.* **2007**, *126*, 144109.
(25) Jiang, W.; Hodoscek, M.; Roux, B. *J. Chem. Theory Comput.* **2009**, *5*, 2583–2588.
(26) Jiang, W.; Roux, B. *J. Chem. Theory Comput.* **2010**, *6*, 2559–2565.
(27) Dyson, H. J.; Tennant, L. L.; Holmgren, A. *Biochemistry* **1991**, *30*, 4262–4268.
(28) Langsetmo, K.; Fuchs, J. A.; Woodward, C. *Biochemistry* **1991**, *30*, 7603–7609.
(29) Christ, C. D.; Mark, A. E.; van Gunsteren, W. F. *J. Comput. Chem.* **2010**, *31*, 1569–1582.
(30) Jorgensen, W. L.; Thomas, L. L. *J. Chem. Theory Comput.* **2008**, *4*, 869–876.
(31) Kollman, P. *Chem. Rev.* **1993**, *93*, 2395–2417.
(32) Straatsma, T. P.; Mccammon, J. A. *Annu. Rev. Phys. Chem.* **1992**, *43*, 407–435.
(33) Jorgensen, W. L.; Ravimohan, C. *J. Chem. Phys.* **1985**, *83*, 3050–3054.
(34) Lu, N. D.; Kofke, D. A.; Woolf, T. B. *J. Comput. Chem.* **2004**, *25*, 28–39.
(35) Metropolis, N.; Rosenbluth, A. W.; Rosenbluth, M. N.; Teller, A. H.; Teller, E. *J. Chem. Phys.* **1953**, *21*, 1087–1092.
(36) Simonson, T.; Carlsson, J.; Case, D. A. *J. Am. Chem. Soc.* **2004**, *126*, 4167–4180.
(37) Bashford, D.; Case, D. A.; Dalvit, C.; Tennant, L.; Wright, P. E. *Biochemistry* **1993**, *32*, 8045–8056.
(38) Katti, S. K.; Lemaster, D. M.; Eklund, H. *J. Mol. Biol.* **1990**, *212*, 167–184.
(39) Case, D. A.; Darden, T. A.; Cheatham, T. E.; Simmerling, C. L.; Wang, J.; Duke, R. E.; Luo, R.; Crowley, M.; Walker, R. C.; Zhang, W.; Merz, K. M.; B.;, W.; Hayik, S.; Roitberg, A. E.; Seabra, G.; Kolossváry, I.;

Wong, K. F.; Paesani, F.; Vanicek, J.; Brozell, S. R.; Steinbrecher, T.; Gohlke, H.; Yang, L.; Tan, C.; Mongan, J.; Hornak, V.; Cui, G.; Mathews, D. H.; Seetin, M. G.; Sagui, C.; Babin, V.; Kollman, P. A. *AMBER 10*; University of California: San Francisco, 2008.

(40) Hornak, V.; Abel, R.; Okur, A.; Strockbine, B.; Roitberg, A.; Simmerling, C. *Proteins: Struct., Funct., Bioinf.* **2006**, *65*, 712–725.

(41) Ryckaert, J. P.; Ciccotti, G.; Berendsen, H. J. C. *J. Comput. Phys.* **1977**, *23*, 327–341.

(42) Onufriev, A.; Case, D. A.; Bashford, D. *J. Comput. Chem.* **2002**, *23*, 1297–1304.